Hydrolysis of Chemically Distinct Sites of Human Serum Albumin (HSA) by Polyoxometalate (POM): A Hybrid QM/MM (ONIOM) Study

J. A. Vindi Mahesha[§], Qiaoyu Hu[§], Gaurav Sharma[§], Thomas J. Paul[§], Marcus Lundberg[†], David Quiñonero[‡], Tatjana N. Parac-Vogt[Δ] and Rajeev Prabhakar[§,*]

§ *Department of Chemistry, University of Miami, Coral Gables, FL 33146*

† *Department of Chemistry - Ångström Laboratory, Uppsala University, 751 21 Uppsala, Sweden*

‡ *Department of Chemistry, Universitat de les Illes Balears, Palma de Mallorca, Spain*

Δ *Department of Chemistry, KU Leuven, Leuven, Belgium*

Dedicated to the Memory of Prof. Keiji Morokuma

* To whom correspondence should be addressed; rpr@miami.edu; Tel: 305-284-9372; Fax: 305-284-4571.

Abstract

In this study, mechanisms of hydrolysis of all four chemically diverse cleavage sites of Human Serum Albumin (HSA) by $[Zr(OH)(PW_{11}O_{39})]^{4-}$ (ZrK) have been investigated using the hybrid two-layer QM/MM (ONIOM) method. These reactions have been proposed to occur through the following two mechanisms: internal attack (IA) and water assisted (WA). In both mechanisms, the cleavage of the peptide bond in the Cys392-Glu393 site of HSA is predicted to occur in the rate-limiting step of the mechanism. With the barrier of 27.5 kcal/mol for the hydrolysis of this site, the IA mechanism is found to be energetically more favorable than the WA mechanism (barrier = 31.6 kcal/mol). The energetics for the IA mechanism are in line with the experimentally measured values for the cleavage of a wide range of dipeptides. These calculations also suggest an energetic preference (Cys392-Glu393, Ala257-Asp258, Lys313-Asp314, and Arg114-Leu115) for the hydrolysis of all four sites of HSA.

Keywords: Polyoxometalates, Human Serum Albumin, Peptide Hydrolysis, Reaction Mechanism, QM/MM (ONIOM) method.

Introduction

Selective peptide hydrolysis is required in a wide range of modern biochemical, biotechnological, and biomedical applications like proteomics,[1] protein engineering[2,3], protein footprinting,[4-10] protein sequencing,[1,11] bioethanol production[12], and catalytic drugs.[13,14] Additionally, a majority of enzymes that are utilized in textile, food, leather, paper and ethanol production industries are peptide hydrolyzing enzymes.[12,15] However, the peptide or amide bond is exceptionally stable and the half-life of its uncatalyzed hydrolysis is 350-600 years at room temperature and in a pH range of 4-8.[16-18] In the last couple of decades, intense efforts have been made to design metal complexes such as polyoxometalates (POMs) for efficient peptide hydrolysis under mild conditions.[13,19-60] However, currently only a few metal complexes can efficiently catalyze peptide hydrolysis in a regioselective manner under mild conditions.[55,61] For instance, aqueous solutions of Zr(IV) form precipitates and inactive gels at neutral and basic pH values.[62-64] On the other hand, POMs have been reported to selectively catalyze hydrolysis of a wide range of critical biomolecules such as human serum albumin (HSA),[58,59] hen egg-white lysozyme (HEWL)[65], myoglobin[1,66], b-insulin[66] and cytochrome c.[67] These metal clusters utilize their remarkable chemical properties like charge, oxidation state, and ligand environment to catalyze these reactions.[58,68,69,70-77] On the other hand, the HSA protein has been commonly used to explore the physicochemical basis of drug-protein interactions.[78] It is one of the major soluble constituents of the circulatory system and contributes significantly to metabolism of ligands.[79-81] Recently, HSA has been reported to be hydrolyzed by a variety of POMs $[(nBu_4N)_5[\{W_5O_{18}Zr(\mu\text{-}OH)\}_2].2H_2O$ (Zr2-L2), $(Et_2NH_2)_{10}[Zr(PW_{11}O_{39})_2].7H_2O$ (Zr1-K2), $(Et_2NH_2)_8[\{\alpha\text{-}PW_{11}O_{39}Zr(\mu\text{-}OH)(H_2O)\}_2].7H_2O$ (Zr2-K2), and $K_{15}H$ $[Zr(\alpha_2\text{-}P_2W_{17}O_{61})_2].25H_2O$ (Zr1-WD2)] at 60 °C and pH 7.4.[58] For instance, Zr-containing Keggin POM (Zr1-K2) was found to hydrolyze less than 35% of HSA after 48 hours,

but the degree of hydrolysis was substantially enhanced after 192 hours.[58] However, instead of dimeric (1:2) Zr1-K2, the monomeric 1:1 (ZrK) form of this POM was identified as the reactive species in the hydrolysis.[82,83] The Zr1-K2 to ZrK transformation has also been reported to be assisted by the protein environment and after its formation ZrK is stabilized by electrostatic and water-mediated hydrogen bonding interactions with the protein.[84] Additionally, Eu(III) luminescence spectroscopy provided evidence of this transformation at physiological pH and low POM concentrations in the presence of HSA (Figure 1).[85] Furthermore, a co-crystal structure of monomeric ZrK with another biomolecule (HEWL) was resolved recently.[86]

ZrK exhibited its versatility by hydrolyzing multiple peptide bonds of HSA in a rather non-preferential manner. In particular, it hydrolyzed four chemically diverse bonds: Arg114-Leu115 (site 1), Ala257-Asp258 (site 2), Lys313-Asp314 (site 3), and Cys392-Glu393 (site 4) of HSA formed by distinct amino acid residues i.e. polar charged (Arg, Asp and Glu) and nonpolar neutral (Leu, Ala and Cys) (Figure 1).[58] The measured rate constants of these reactions are not available. The last site (site 4) has been reported as the major binding site for a wide range of drug molecules like ibuprofen[87,88] and diazepam[89,90]and is known as Sudlow's drug site 2.[91,92] Competition experiments have shown that the addition of ibuprofen inhibited interaction of POMs with HSA and resulted in lower protein hydrolysis, further confirming the preferential binding of POM at site 4.[58] Interestingly, addition of warfarin, which is known to bind to drug site 1 of HSA, did not show any effect on the binding of POMs nor on the HSA hydrolysis. Warfarin binding has been suggested to occur in the apolar core region of the protein, where the few polar contacts are not solvent accessible to the extent to allow for efficient POM binding.[58] However, ZrK needs to bind adjacent to the cleavage sites of HSA for its activity.[65] The required ZrK-substrate complexation

is suggested to be steered by either the binding of the Zr ion of ZrK to the side chains of amino acid residues of HSA or electrostatic interactions between the negative charges of oxygen atoms of ZrK and positive charges of residues of HSA.[93-98] The metal ion has been known to play key roles in peptide hydrolysis by metal complexes.[55,99-111] It functions as a Lewis acid and activates a nucleophile in the reaction.[13,55,101,107,109,112,113] Additionally, this ion has been proposed to play similar roles in the hydrolysis of esters, phosphoesters and nitriles.[13,104,105,114-127] The Zr ion of ZrK also exhibits significant hydrolytic activity, due to its properties like high Lewis acidity, redox stability and oxophilicity.[35,55,128-133] Additionally, it displays fast ligand exchange kinetics, and is kinetically and stereochemically labile.[134-136] The measured rate constants at pD (pH+0.41) 5.4 and 60 °C for the hydrolysis of 18 different dipeptides by Zr1-K2 were in the range of (0.72-63.33) × 10^{-7} s^{-1},[137] which corresponds to barriers between (24.5-27.0) kcal/mol using Arrhenius equation with the pre-exponential factor of 10^{13}.

The ZrK catalyzed peptide hydrolysis has been proposed to occur via the general dual activation mechanism.[138-140] This mechanism was also proposed to be utilized by metalloproteases such as thermolysin and insulin degrading enzyme.[141,142] According to the mechanism (Figure 2), the binding of the HSA substrate to the ZrK ($\mathbf{R'_E}$) generates the reactant ($\mathbf{R_E}$). In $\mathbf{R_E}$, the Zr ion plays the role of a Lewis acid and activates the HSA substrate through the coordination of its carbonyl oxygen atom. This interaction increases the electrophilicity of the carbonyl carbon atom of the substrate and polarizes the peptide bond. Therefore, the Zr-O=C(HSA) coordination reflects a degree of Lewis acidity of Zr(IV) ion.[143] A weak metal-ligand interaction is also known to increase Lewis acidity of the metal ion.[13,143-146] Since Zr(IV) bound water is known to have very low pK_a value (≤ 0.6), it creates a hydroxyl nucleophile by activating a water molecule.[147] From $\mathbf{R_E}$, an

attack of the hydroxyl nucleophile on the amide carbonyl carbon of HSA generates a four-membered ring containing tetrahedral intermediate ($\mathbf{IN_E}$). In this process, the Zr(IV) ion facilitates the release of the nucleophile at the peptide bond due to the fast ligand exchange kinetics.[136] The Zr(IV)-OH bond distance provides a measure of the strength of the nucleophile.[45,148] Lewis acidity of the Zr(IV) ion and nucleophilicity of the hydroxyl ion along with geometry of $\mathbf{IN_E}$ influence the kinetics of this step.[140] The first two effects can counter each other i.e. an increase in Lewis acidity of the metal ion can lower the nucleophilicity of the hydroxyl ion.[143,149-152] In the last step, a proton transfer from the hydroxyl ion to the amine group of HSA splits the amide bond (-C-N-). Here, the Zr(IV) ion promotes the release of separated amine ($-NH_2$) and carboxyl (-COO) termini ($\mathbf{P_E}$).

Despite the wealth of experimental information available, the exact mechanism, rate constants, and structures for the hydrolysis of all four sites of HSA by ZrK are not known. In this two layer QM/MM (ONIOM) study, we have elucidated the mechanistic, kinetic and structural properties of HSA hydrolysis at multiple sites by ZrK. The results reported in this study will contribute to the design of the next generation of POMs with improved metalloproteases like activities. They may also provide interesting insights into designing metal complexes to catalyze hydrolysis of phosphoesters, nitriles and other reactions including epoxide opening, aldol condensation, Michael addition, and Diels-Alder reactions.

Computational Details

Methods: Since it is still not possible to treat the entire ZrK-HSA complex using pure quantum mechanics (QM), we employed the hybrid QM/MM (ONIOM) approach in this study. All ONIOM calculations including optimization of reactants, transition states, intermediates and products were

performed using the Gaussian 09 program package.[153] This method allows treatment of a large system in a simple and accurate manner. In comparison to other QM/MM methods, it does not require explicit QM-MM coupling terms and the bond between the QM and MM regions is treated using the link atom method.[154] ONIOM is a subtractive method in which the MM energy [E_{MM} (model)] of the QM (model) part is subtracted from the sum of the QM energy of the model [E_{QM} (model)] and MM energy [E_{MM} (real)] of the whole (real) system i.e. E_{ONIOM}(QM/MM) = E_{QM} (model) + E_{MM} (real) - E_{MM} (model). This subtraction corrects the artifacts introduced by the link atom. The details and applications of this method were reviewed recently.[155] In these calculations, the system was divided into two parts. A selected model system [ZrK (POM), and the cleavage site (Arg114-Lue115 / Ala257-Asp258/ Lys313-Asp314 / Cys392-Glu393)] where the chemical reactions occur was treated with quantum mechanics (QM, a high-level method), while the remaining part of the HSA substrate was treated with molecular mechanics (MM, a low-level method). The ONIOM optimization procedure uses macro/microiterations[156] and the electrostatic interactions between the QM and the MM part were treated by mechanical embedding (ME). The geometries in the QM part were optimized without any symmetry constraints at the B3LYP/Lanl2dz level of theory[157,158] [With corresponding Hay-Wadt effective core potential (ECP) for Zr, and W[159]], and the 6-31G(d) basis set was used for all the other atoms in QM layer. The MM part was treated using the AMBER force field.[160,161] The final energies of the optimized structures were further improved by performing single-point calculations using 6-311+G(d,p) basis set for P and S, Lanl2dz for W and Zr along with 6-31G(d) for all the other atoms in the QM layer. The treatment of Zr with larger [Lanl2tz (+)] basis set made only a minor effect (less than 1.0 kcal/mol) on the computed energies.

Hessians were calculated at the same level of theory as the optimizations to confirm the nature of the stationary points along the reaction coordinate. Zero-point vibrational (unscaled), thermal (at 298.15 K and 1 atm), and entropy corrections (at 298.15 K) were added to the final energies of the optimized structures. Transition states were confirmed to have only one imaginary frequency corresponding to the reaction coordinate. One well known problem with QM/MM optimizations is the iterative nature of these methods that tend to maximize interactions in the MM part. In some cases, these changes in conformational space might not be connected with the actual reaction coordinates. Therefore, while comparing energies of different minima and saddle points in the potential energy surface, we localized the corresponding transition state and minima, back and forth, to make sure that these points are connected with each other.

Models: The structures of ZrK and HSA were obtained from the Protein Data Bank (PDB ID: 4XYY and 4K2C, respectively).[162,163] The starting structures of all ZrK-HSA complexes were taken from our previous Molecular Dynamic (MD) simulations. In the models, the entire ZrK cage and dipeptide cleavage site, e.g. Cys392-Glu393 for site 4, of HSA are included in the QM layer, while the remaining HSA constitutes the MM layer. All water molecules that do not directly participate in hydrolysis are also included in the MM layer. The total number of atoms in the ZrK-HSA complex is 9197 including 77-97 atoms in the QM layer (varies from site to site) and remaining in the MM layer. The total number of atoms in the LW model including water molecules (shown in parenthesis) for site1 (122), 2 (94), 3 (54) and 4 (57) are 9563, 9482, 9353 and 9368, respectively. The charge on the ZrK is -4 and the total charge for all ZrK-HSA complexes is -18. All structures exist in the singlet spin state.

Results and Discussion

In this QM/MM (ONIOM) study, the hydrolytic cleavage of HSA is investigated using two different mechanisms i.e. internal attack (IA) and water assisted (WA), Figure 3.[105,139] Since the cleavage sites of the substrate are exposed to water, the effect of the solvent on the computed energetics was investigated using the following two models: (1) no water in the low layer (NW), and (2) 57 explicit waters in the low layer (LW). Based on the available experimental data, both these mechanisms were first employed to study the hydrolysis of the major binding site (Cys392-Glu393, site 4) of HSA. The most energetically favorable mechanism suggested by these calculations was subsequently used to investigate the hydrolysis of the remaining three sites.

Hydrolysis of site 4 through the internal attack (IA) mechanism.

Internal attack (IA) mechanism (NW Model): In the reactant ($\mathbf{R_{NW}}$) of this mechanism, the Zr(IV) ion is coordinated to a hydroxyl group, and five oxygen atoms of the POM cage in a distorted octahedral conformation (Zr-O^p = 1.96 Å in Figure 4). In $\mathbf{R_{NW}}$, the carbonyl oxygen atom of the scissile peptide bond (Cys392-Glu393) of HSA does not directly coordinate to the Zr(IV) ion of ZrK (Zr-O^S = 4.16 Å, C^S-O^S=1.23 Å, C^S-N^S = 1.37 Å, C^S-O^P = 2.88 Å, Table S1). The missing Zr-O^S coordination suggests that the Lewis acidity of the Zr ion is not critical in this step. The ZrK-HSA complex is instead held together by a network of hydrogen bonds and electrostatic interactions. The Zr-bound hydroxyl (-O^PH^P) nucleophile interacts through two moderately strong hydrogen bonds (2.81 Å and 2.41 Å) with the carbonyl oxygen (O^S) atom and the nitrogen (N^S) atom of the Cys392-Glu393 cleavage site of HSA, respectively. Additionally, twelve other inter

molecular hydrogen bonds between the oxygen atoms of ZrK and amino acid residues of HSA stabilize this complex. Moreover, electrostatic interactions between the positively charged N-terminal of Lys389 and Lys402 and negatively charged oxygen atoms of ZrK provide further stabilization.

In the first step, the Zr(IV) bound hydroxyl ($-O^PH^P$) group makes a nucleophilic attack on the electrophilic carbon (C^S) of the scissile peptide bond. This process occurs with a barrier of 23.3 kcal/mol and the optimized transition state (**$TS1_{NW}$**) is shown in Figure 4. In **$TS1_{NW}$**, the Zr(IV) ion is bound to the carbonyl oxygen (O^S) of the peptide bond. Here, the electrophile-nucleophile (C^S-O^P) distance is decreased by 1.05 Å and the metal-nucleophile (Zr-O^P) bond is elongated by 0.25 Å in comparison to **R_{NW}** (Zr-O^S = 2.23 Å, C^S-O^P = 1.83 Å and Zr-O^P = 2.21 Å). This transition state is also stabilized by two moderately strong hydrogen bonds contributed by the HSA substrate. The nucleophilic attack in this step leads to the formation of a tetrahedral intermediate (**IN_{NW}**). In **IN_{NW}**, the peptide bond is significantly activated by 0.05 Å and both O^P and O^S atoms are bound to the Zr ion (C^S-N^S= 1.42 Å, Zr-O^P = 2.43 Å, and Zr-O^S = 2.12 Å). This intermediate is further stabilized by four hydrogen bonds between ZrK and HSA (O^S-H^P =2.93 Å, N^S-H^P =2.39 Å, NH-O^P =2.84 Å, and 3.05 Å, Table S1). The formation of **IN_{NW}** is endothermic by 13.6 kcal/mol from **R_{NW}**. This intermediate is calculated to be endothermic in the mechanisms of other metal complexes as well.[108-111,164,165]

In the next step, from **IN_{NW}**, a transfer of the H^P proton of the hydroxyl nucleophile to the N^S atom of the peptide bond (C^S-N^S) leads to its cleavage. This process takes place with a barrier of 21.8 kcal/mol from **IN_{NW}** and the optimized transition state (**$TS2_{NW}$**) is shown in Figure 4. All key

distances in **TS2$_{NW}$** indicate the synchronized nature of this transition state (O^P-H^P = 1.24 Å, N^S-H^P = 1.34 Å, and C^S-N^S = 1.59 Å). Furthermore, one hydrogen bond between O^S-H^P (2.72 Å) and two hydrogen bonds between the NH groups of the substrate (2.15 Å, and 3.05 Å) provide additional stability to **TS2$_{NW}$**. Since this step followed a step that was endothermic by 13.6 kcal/mol, the overall barrier from **R$_{NW}$** became 35.4 kcal/mol. This is computed to be the rate-limiting step of the entire mechanism. This result is also supported by the computed energetics of other metal complexes.[108-111,164,165] This process leads to the creation of the HSA bound separated neutral amine (-NH_2) and charged carboxylate (-COO^-) groups in the final product (**P$_{NW}$**). The formation of **P$_{NW}$** is exothermic by 48.9 kcal/mol from **R$_{NW}$**.

These calculations suggest that the Lewis acid activation of the substrate does not play an important role in this mechanism but rather is dominated by the nucleophilicity of the Zr-bound hydroxyl ion.

Internal attack (IA) mechanism (LW Model): Here, the previous IA mechanism is investigated by including 57 explicit solvent water molecules in the low layer of the QM/MM (ONIOM) calculations (LW model in Figure 5). In the reactant (**R$_{LW}$**) of this model, unlike **R$_{NW}$**, the Zr(IV) ion weakly interacts with the carbonyl oxygen (O^S) atom of the scissile Cys392-Glu393 peptide bond of HSA (Figure 5). In comparison to **R$_{NW}$**, the Zr-nucleophile coordination becomes slightly weaker by 0.05 Å in **R$_{LW}$** (Zr-O^P = 2.01 Å). However, both hydrogen bonds between the nucleophile and the substrate that were also present in **R$_{NW}$** remained intact. Additionally, seven other intermolecular hydrogen bonds and multiple electrostatic interactions along with water mediated interaction between the ZrK cage and the substrate provide extra stabilization to **R$_{LW}$**.

The barrier for the first step in this LW model is 5.0 kcal/mol lower than the one computed using the previous NW model i.e. 18.3 kcal/mol from $\mathbf{R_{LW}}$. In the optimized transition state ($\mathbf{TS1_{LW}}$), the Zr-O^P bond distance becomes longer by 0.28 Å and increases the nucleophilicity of the hydroxyl group (-O^PH^P). Here, the Zr-HSA interaction also becomes stronger (Zr-O^S = 2.22 Å). Thus, the computed reduction in barrier for the LW model is most likely caused by the increased strength of the nucleophile and extra stabilization provided by additional hydrogen bonds (H^P-N^S = 2.42 Å, H^P-NH =3.08 and NH-NH = 2.13 Å, 2.70 Å, Figure 5 and Table S1). The intermediate ($\mathbf{IN_{LW}}$) formed in this step is also 5.6 kcal/mol more stable than $\mathbf{IN_{NW}}$. In $\mathbf{IN_{LW}}$, the activated peptide bond (C^S-N^S) is 0.04 Å longer than the one in $\mathbf{IN_{NW}}$. The substrate is also coordinated to ZrK through a stronger Zr-O^S bond (Zr-O^S = 2.08 Å). Moreover, an extra hydrogen bond (2.70 Å) between ZrK and the HSA substrate in the high layer further stabilizes this intermediate. The cleavage of the peptide bond in the rate-limiting step using this model occurs with a significantly (7.9 kcal/mol) lower barrier (27.5 kcal/mol from $\mathbf{R_{LW}}$) than the barrier using the NW model. This barrier is in excellent agreement with the measured barrier of 24.5-27.0 kcal/mol for the hydrolysis of 18 different dipeptides by Zr1-K2.[137] However, these dipeptides were different from the cleavage sites of HSA. It is substantially lower than the computed barriers for other metal complexes such as metal (Co and Cu)-cyclen and $[Pd(H_2O)_4]^{2+}$ [108-111,164,165] but higher than the barrier for a natural metalloprotease, Insulin degrading enzyme (IDE)[166]. However, from the tetrahedral intermediate ($\mathbf{IN_{LW}}$), the barrier for the cleavage of the peptide bond in this step is only 2.3 kcal/mol lower than the barrier in the NW model. The differences in the key bond distances in transition states ($\mathbf{TS2_{NW}}$ and $\mathbf{TS2_{LW}}$) for this step contribute to this difference. In comparison to $\mathbf{TS2_{NW}}$, the O^P-H^P bond is slightly longer by 0.03 Å, and the N^S-H^P bond is shorter by 0.04 Å in $\mathbf{TS2_{LW}}$ (O^P-H^P = 1.27 Å, N^S-H^P = 1.30 Å, and C^S-N^S = 1.56 Å, Figure 5). Additionally, a 0.03 Å

shorter Zr-O^S (2.16 Å) bond length suggests stronger Lewis acidity of the Zr ion. Furthermore, like all other maxima and minima on this potential energy surface, the final product in the LW model ($\mathbf{P_{LW}}$) is ~17.0 kcal/mol lower in energy than $\mathbf{P_{NW}}$. The presence of two moderately strong hydrogen bonds, water mediated interactions and tighter binding of the separated C- and N- termini contribute to the higher exothermicity of this product.

These calculations suggest that the nucleophilicity is more dominant than Lewis acidity in the mechanism. The cleavage of peptide bond occurs in the rate-limiting step (barrier = 27.5 kcal/mol) of the IA mechanism, which is line with the available data. The LW model is found to be more accurate than the NW model to investigate this mechanism.

Water assisted (WA) mechanism (LW model): In the water assisted (WA) mechanism, an external water molecule ($H^1O^WH^2$) hydrogen bonded to the Zr-bound hydroxyl is utilized for the hydrolysis (Figure 6). The same number of explicit water molecules, as used in the previous LW model, are included in the MM layer for this mechanism.

In the reactant $\mathbf{R_{WA}}$, the water molecule ($H^1O^WH^2$) bridges the Zr-hydroxyl and the cleavage site of HSA through two hydrogen bonds (Figure 6). Similar to the reactant in the IA mechanism ($\mathbf{R_{LW}}$), the substrate does not directly interact with the Zr ion through a coordination to the carbonyl oxygen (O^S). In $\mathbf{R_{WA}}$, there are multiple direct and water mediated hydrogen bonds between the ZrK cage and Glu393, Arg410, Lys 389 and Lys402 residues of HSA. In the first step of the mechanism, the Zr(IV) bound hydroxyl group (-O^PH^P) in $\mathbf{R_{WA}}$ functions as a base and abstracts the H^2 proton of the external water ($H^1O^WH^2$) molecule. The resulting hydroxyl group (-

O^WH^1) generated in this process acts as a nucleophile and attacks the C^S atom of the substrate. This process takes place with a barrier of 26.6 kcal/mol and all the key distances in the optimized transition state (**TS1$_{WA}$**) indicate its synchronous nature (Zr-O^S = 2.30 Å, H^2-O^P = 1.04 Å and C^S-O^W = 1.97 Å, Table S1). The barrier for this step is 8.3 kcal/mol higher than the one computed for the previous IA mechanism. The reason for this significant increase is the activation of a hydrogen bonded water molecule ($H^1O^WH^2$) here. This water, although trapped through hydrogen bonding, possesses a very high pK_A value and there is a substantial energetic penalty associated with its activation. In the tetrahedral intermediate (**IN$_{WA}$**) created in this process, a water molecule is bound to the Zr(IV) ion and the peptide bond is significantly (0.09 Å) activated (C^S-N^S= 1.46 Å). This water molecule interacts via three hydrogen bonds with the HSA substrate. Like the transition state (**TS1$_{WA}$**), **IN$_{WA}$** is substantially (7.7 kcal/mol) higher in energy than the intermediate (**IN$_{LW}$**) formed in the IA mechanism.

From **IN$_{WA}$**, the cleavage of the scissile peptide bond (C^S-N^S) through the abstraction of the H^1 proton from the C^S-O^WH^1 group occurs with an overall barrier of 31.6 kcal/mol from **R$_{WA}$**. This barrier is 4.1 kcal/mol higher than the barrier computed in the IA mechanism. As another possibility, the cleavage of the C^S-N^S bond by the abstraction of H^P proton with concomitant transfer of the H^2 proton to the O^W is also explored. Since the transition state on this path is 16 kcal/mol higher than $TS2_{WA}$, it is ruled out (Figure S1). The final product **P$_{WA}$** in the WA mechanism is exothermic by 59.9 kcal/mol from the reactant **R$_{WA}$**. The generation of **P$_{WA}$** is 6.1 kcal/mol less favorable than the creation of **P$_{LW}$**. Since **P$_{WA}$** and **P$_{LW}$** are structurally different, this energy difference is not surprising. In **P$_{WA}$**, a water molecule and C-terminal of the cleavage site

is bound in a monodentate fashion to the Zr ion, while the C-terminal is coordinated in a bidentate manner to the same metal ion in $\mathbf{P_{LW}}$.

All these calculations suggest that the IA mechanism is energetically more feasible than the WA mechanism. The computed energetics of the former is also in line with the measured rates.[137] Therefore, only the IA mechanism using the more accurate LW model is utilized to study the cleavage of the remaining three sites (site 1, 2 and 3) in the next section.

Hydrolysis of sites 1, 2 and 3 through the IA mechanism (LW model): In the models used for these chemically distinct sites [Arg114-Leu115 (site 1), Ala257-Asp258 (site 2), Lys313-Asp314 (site 3), and Cys392-Glu393 (site 4)], the number of explicit water molecules included in the low layer in the LW model varies from site to site. It depends on the size and microenvironment of the cleavage site. In comparison to 57 water molecules in the reactant ($\mathbf{R_{LW}}$) of site 4, there are 122, 94 and 52 water molecules in the reactants ($\mathbf{R_{LW1}}$, $\mathbf{R_{LW2}}$, and $\mathbf{R_{LW3}}$) for sites 1, 2 and 3, respectively. Despite the overall similarity in the structures of these reactants, there are some key differences that can be associated with their distinct reactivities. In $\mathbf{R_{LW}}$, $\mathbf{R_{LW1}}$, $\mathbf{R_{LW2}}$, and $\mathbf{R_{LW3}}$, the metal-ligand (Zr-O) distance, charge on the Zr(IV) ion and length of the peptide bond (C^S-N^S) are essentially the same (Table S2 and S3). However, the number of key hydrogen bonds in the QM and QM-MM regions are different. In the QM region (2, 3, 1 and 0) and in between QM-MM regions (7, 4, 6 and 4) hydrogen bonds exist in $\mathbf{R_{LW}}$, $\mathbf{R_{LW1}}$, $\mathbf{R_{LW2}}$, and $\mathbf{R_{LW3}}$, respectively. Additionally, the critical metal-nucleophile (Zr-O^P) and metal-substrate (Zr-O^S) interactions in these reactants are substantially different (Zr-O^S = 3.17, 3.59, 3.93 and 2.67 Å and Zr-O^P = 2.01, 2.00, 1.97 and 2.04 Å in $\mathbf{R_{LW}}$, $\mathbf{R_{LW1}}$, $\mathbf{R_{LW2}}$, and $\mathbf{R_{LW3}}$, respectively). These distances provide a

measure of Lewis acidity (Zr-O^S) and strength of nucleophile (Zr-O^P). A comparison of these distances in all four reactants suggests that these two effects are optimized in $\mathbf{R_{LW3}}$. This result is supported by the barrier of 18.3, 19.5, 27.5, and 15.9 kcal/mol from the $\mathbf{R_{LW}}$, $\mathbf{R_{LW1}}$, $\mathbf{R_{LW2}}$, and $\mathbf{R_{LW3}}$, respectively for the nucleophilic attack of the hydroxyl ion (-O^PH^P) on the electrophilic C^S atom in the first step. All optimized transition states ($\mathbf{TS1_{LW}}$, $\mathbf{TS1_{LW1}}$, $\mathbf{TS1_{LW2}}$, and $\mathbf{TS1_{LW3}}$) for this process are shown in Figures S2, S3 and S4, respectively. Although the computed barrier for this step is the lowest for site 3, the tetrahedral intermediate is energetically most favorable for site 4. The generation of this intermediate ($\mathbf{IN_{LW}}$, $\mathbf{IN_{LW1}}$, $\mathbf{IN_{LW2}}$ and $\mathbf{IN_{LW3}}$ (for site 4, 1, 2 and 3, respectively) is endothermic by 8.0, 16.1, 11.0, and 9.4 kcal/mol, respectively from the corresponding reactant. The relative stability of $\mathbf{IN_{LW}}$ among all these intermediates is caused by the shortest Zr-O^S bond (2.08 Å) and the longest Zr-O^P (3.12 Å). Among all four intermediates, the electrophile-nucleophile (C^S-O^P) distance is also the shortest for $\mathbf{IN_{LW}}$ (1.44, 1.51, 1.56 and 1.48 Å for $\mathbf{IN_{LW}}$, $\mathbf{IN_{LW1}}$, $\mathbf{IN_{LW2}}$ and $\mathbf{IN_{LW3}}$, respectively).

From this intermediate, the cleavage of the C^S-N^S peptide bond occurs through the transfer of the H^P proton [C^S-(O^P-H^P)] to the N^S atom. The computed barrier for this process is 19.9 kcal/mol (site 1), 20.0 kcal/mol (site 2), 26.1 kcal/mol (site 3) and 19.5 kcal/mol (site 4) from the corresponding intermediate. The barrier for the cleavage of three sites (site 1, 2 and 4) in this step is quite similar but the barrier for the 3 is higher by approximately 6.0 kcal/mol. This could be due to the loss of 3 hydrogen bonds in the $\mathbf{IN_{LW3}}$ - $\mathbf{TS_{LW3}}$ transition and a slightly weaker (0.01 Å) activation of the peptide bond in the corresponding transition state ($\mathbf{TS2_{LW3}}$). The final product ($\mathbf{P_{LW}}$, $\mathbf{P_{LW1}}$, $\mathbf{P_{LW2}}$ and $\mathbf{P_{LW3}}$ for site 4, 1, 2 and 3, respectively) involving the generation of the separated N- and C-termini is exothermic by 66.0, 60.9, 45.2 and 49.1 kcal/mol, respectively.

These calculations showed that there is a clear energetic preference for the hydrolysis of all four sites of HSA i.e. the hydrolysis of site 4 is the most favorable followed by site 2, 3 and 1.

Summary and Conclusions

In this hybrid QM/MM (ONIOM) study, the mechanism of hydrolytic cleavage of four chemically distinct cleavage sites of Human Serum Albumin (HSA) by $[Zr(OH)(PW_{11}O_{39})]^{4-}$ (ZrK) is investigated. These reactions are studied using two different mechanisms: internal attack (IA) and water assisted (WA). Additionally, two different models (NW and LW) are used to simulate these mechanisms. There is no water in the low layer in the NW model, while 57 explicit water molecules are included in the low layer in the LW model. The potential energy surface (PES) diagrams of these mechanisms are shown in Figure 7 and 8. The computed energetics for the hydrolysis of the major site (site 4) of HSA predicts that the cleavage of the peptide bond occurs in the rate-limiting step (step 2) in both mechanisms. These calculations suggested that the IA mechanism is the energetically most feasible pathway for the hydrolysis of HSA. The barrier using this mechanism in the rate-limiting step is 4.1 kcal/mol lower in energy than the barrier for the WA mechanism for site 4. The LW model is found to be more accurate than the NW model for this mechanism i.e. barrier in the rate limiting step in the former is 7.9 kcal/mol lower than the one in the latter for the same site. The computed energies for the IA mechanism (using the LW model) are in agreement with the measured kinetics for the hydrolysis of 18 different dipeptides.[137] These calculations suggest a clear energetic preference (site 4, site 2, site 3 and site 1) for the hydrolysis of all four sites of HSA by ZrK. In comparison to the Lewis acidity, nucleophilicity is found to be the dominant factor in all these reactions. These results will advance our understanding of peptide

hydrolysis by POMs and pave the way for the design of the next generation of catalysts for this critical process.

Acknowledgements

The authors declare no competing financial interests. This material is based upon work supported by the grant from the National Science Foundation (Grant Number CHE-1664926) to R.P. Computational resources from the Center for Computational Science (CCS) at the University of Miami to R.P. are also greatly appreciated.

Additional Supporting Information including figures (S1-S4) and tables (S1-S3) may be found in the online version of this article.

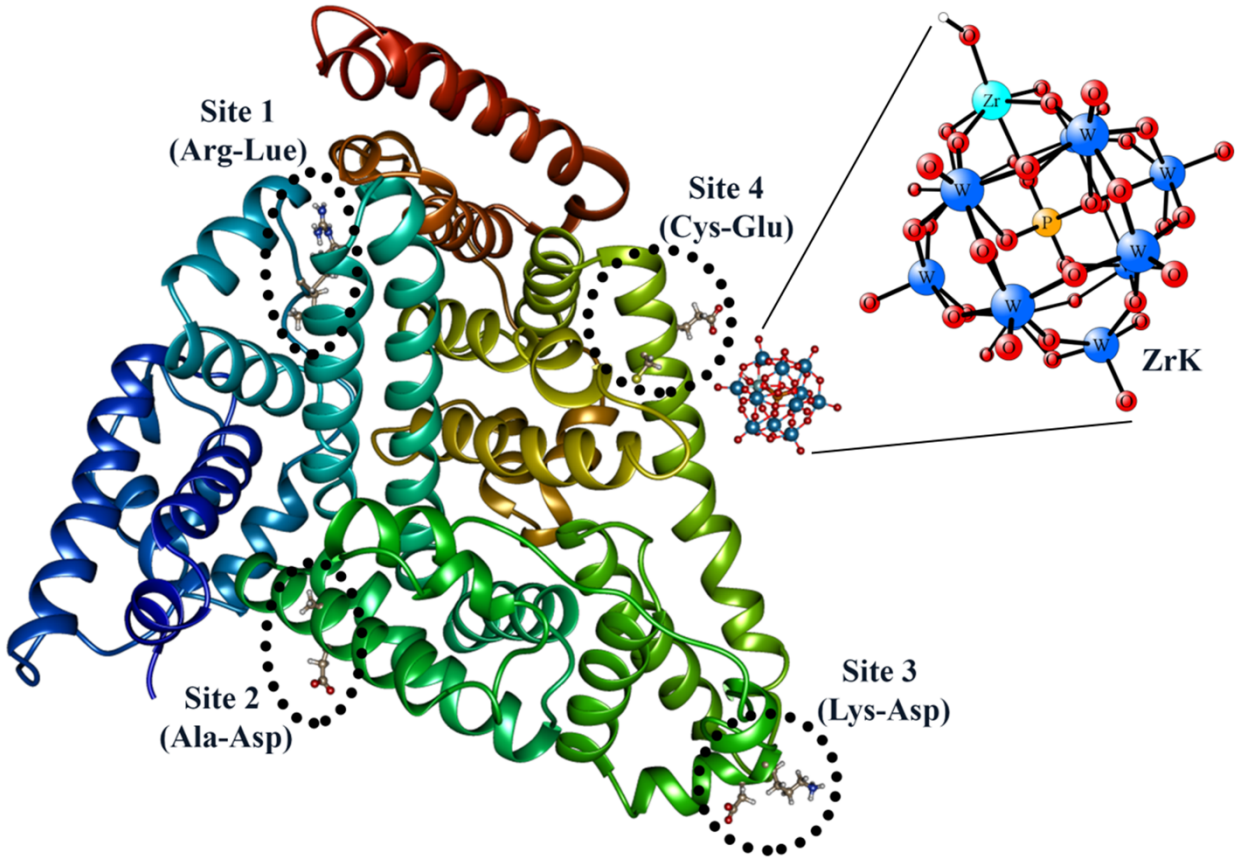

Figure 1: Structure of the polyoxometalate (ZrK) - human serum albumin (HSA) complex. The structures of ZrK and HSA are based on their X-ray structures.[162,163]

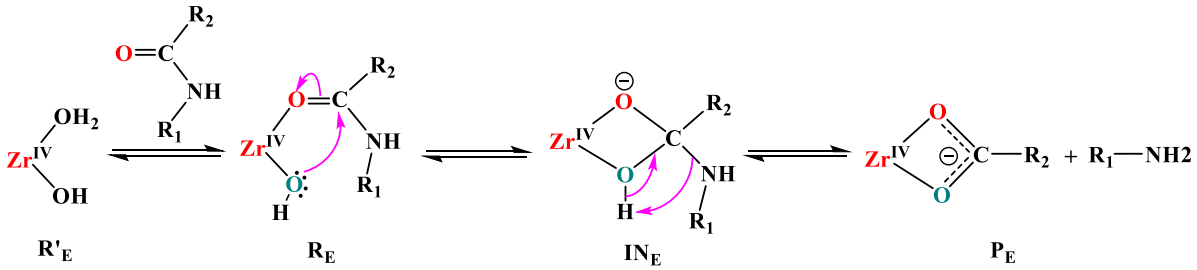

Figure2: The experimentally proposed mechanism for the Zr(IV) assisted peptide hydrolysis.

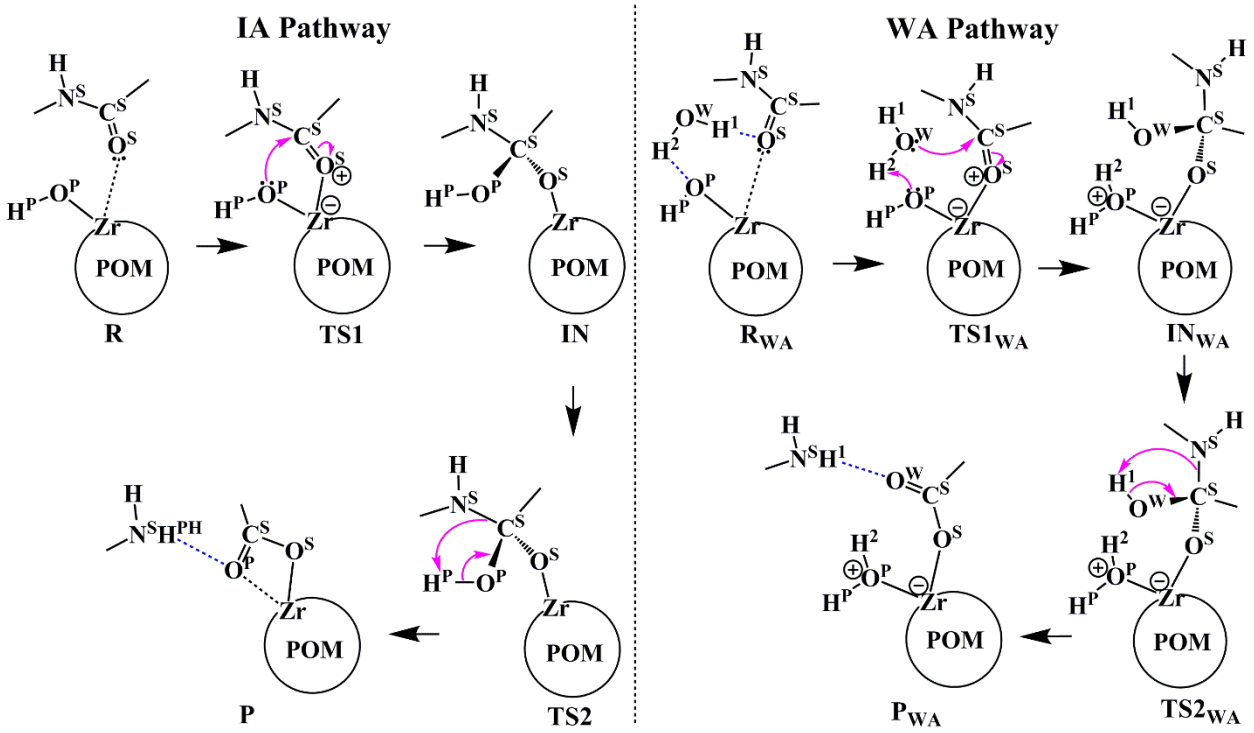

Figure 3: Theoretically studied mechanisms for the HSA hydrolysis by ZrK.[105,139]

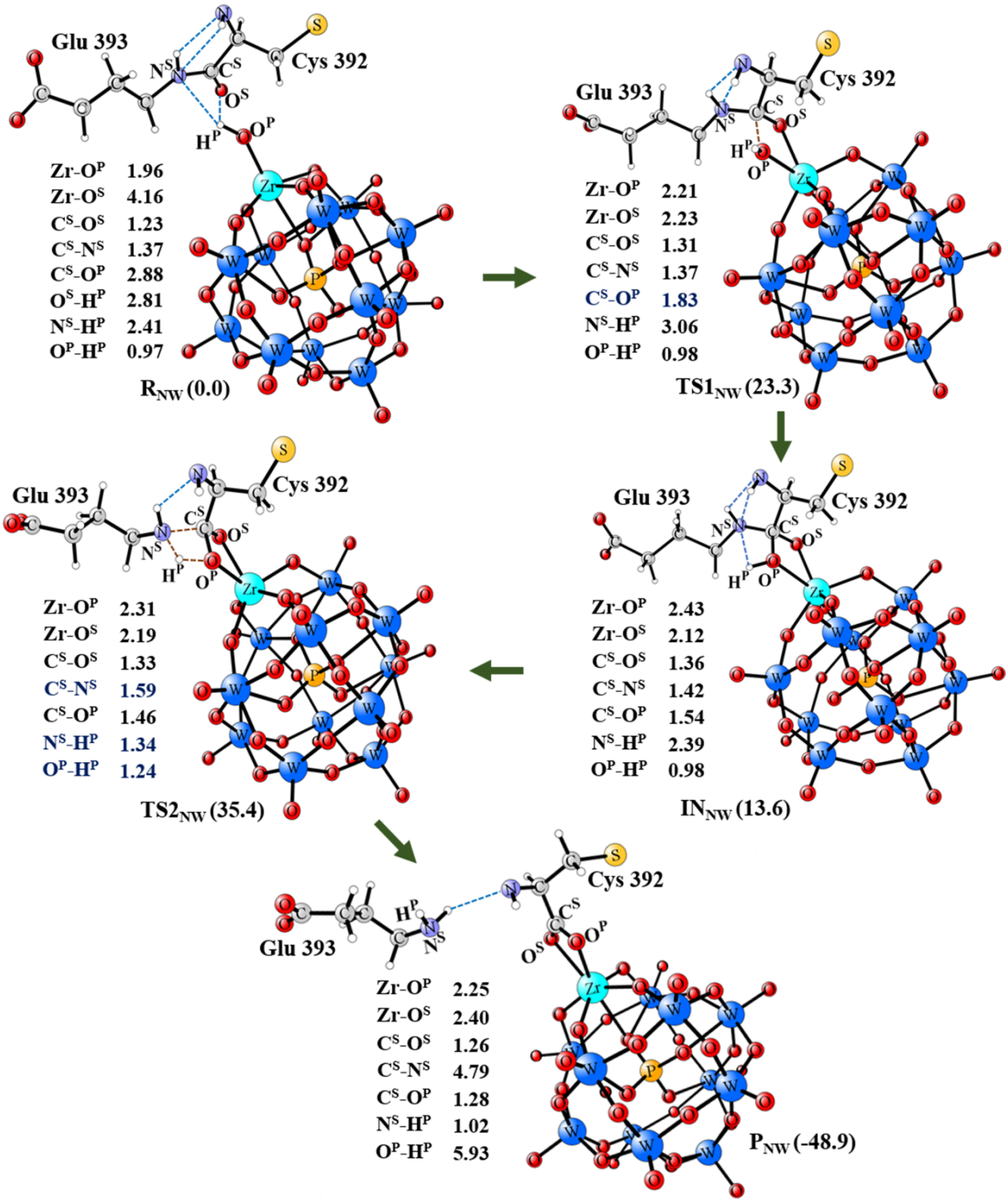

Figure 4: The optimized structures (in Å) and energies (in kcal/mol) for the hydrolysis of site 4 through the IA mechanism (NW Model).

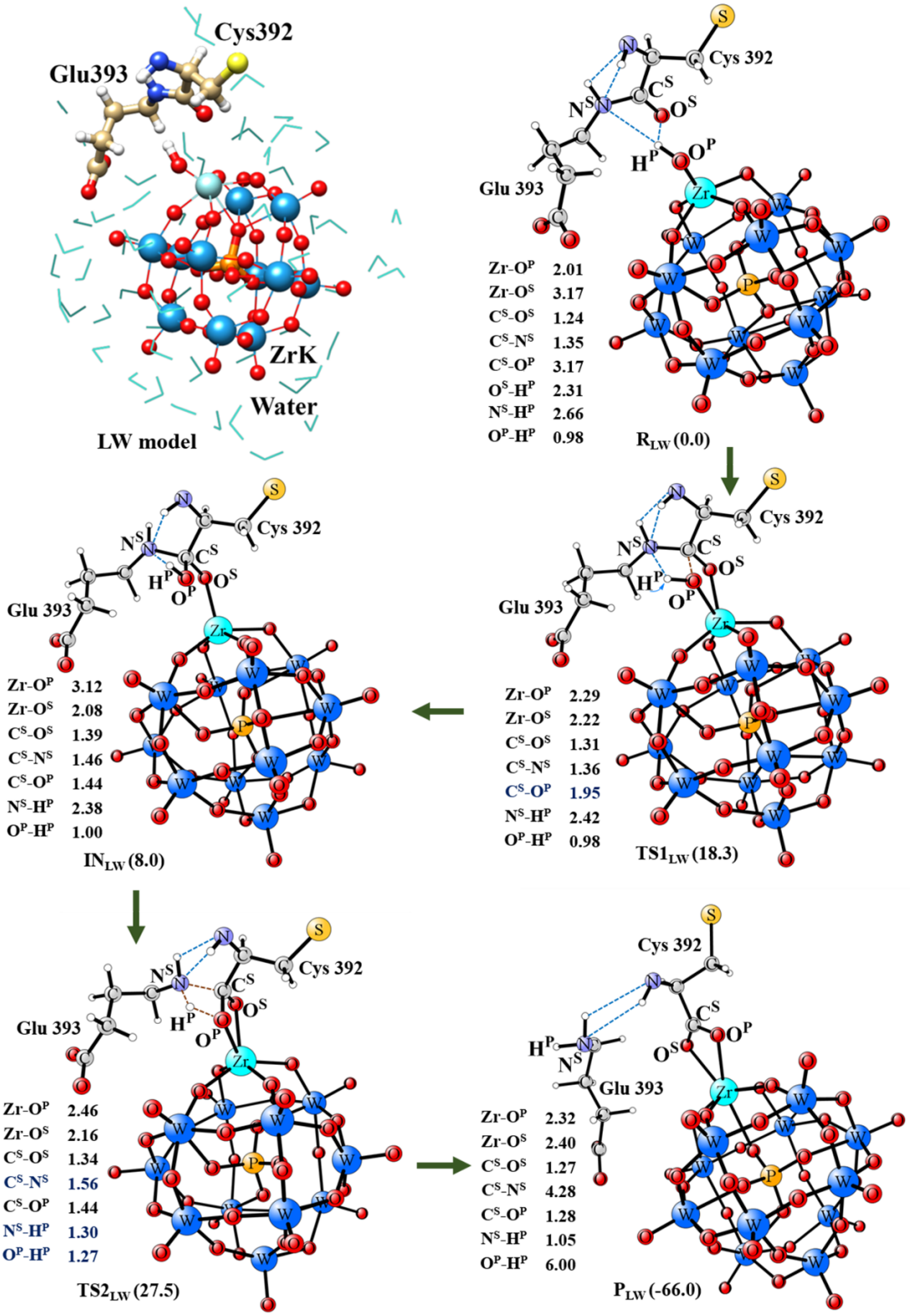

Figure 5: The optimized structures (in Å) and energies (in kcal/mol) for the hydrolysis of site 4 through the IA mechanism (LW model).

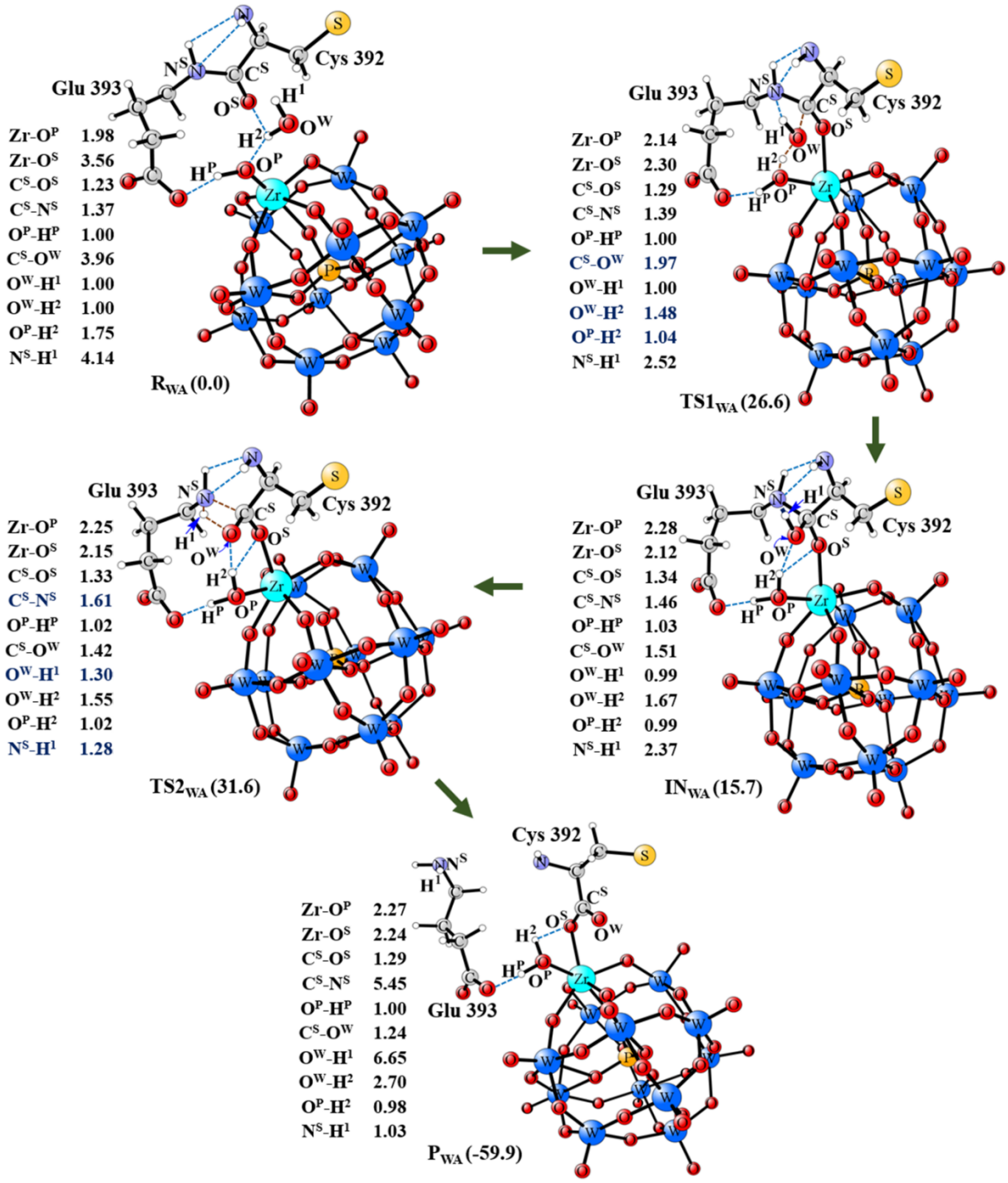

Figure 6: The optimized structures (in Å) and energies (in kcal/mol) for the hydrolysis of site 4 through the AA mechanism (LW model).

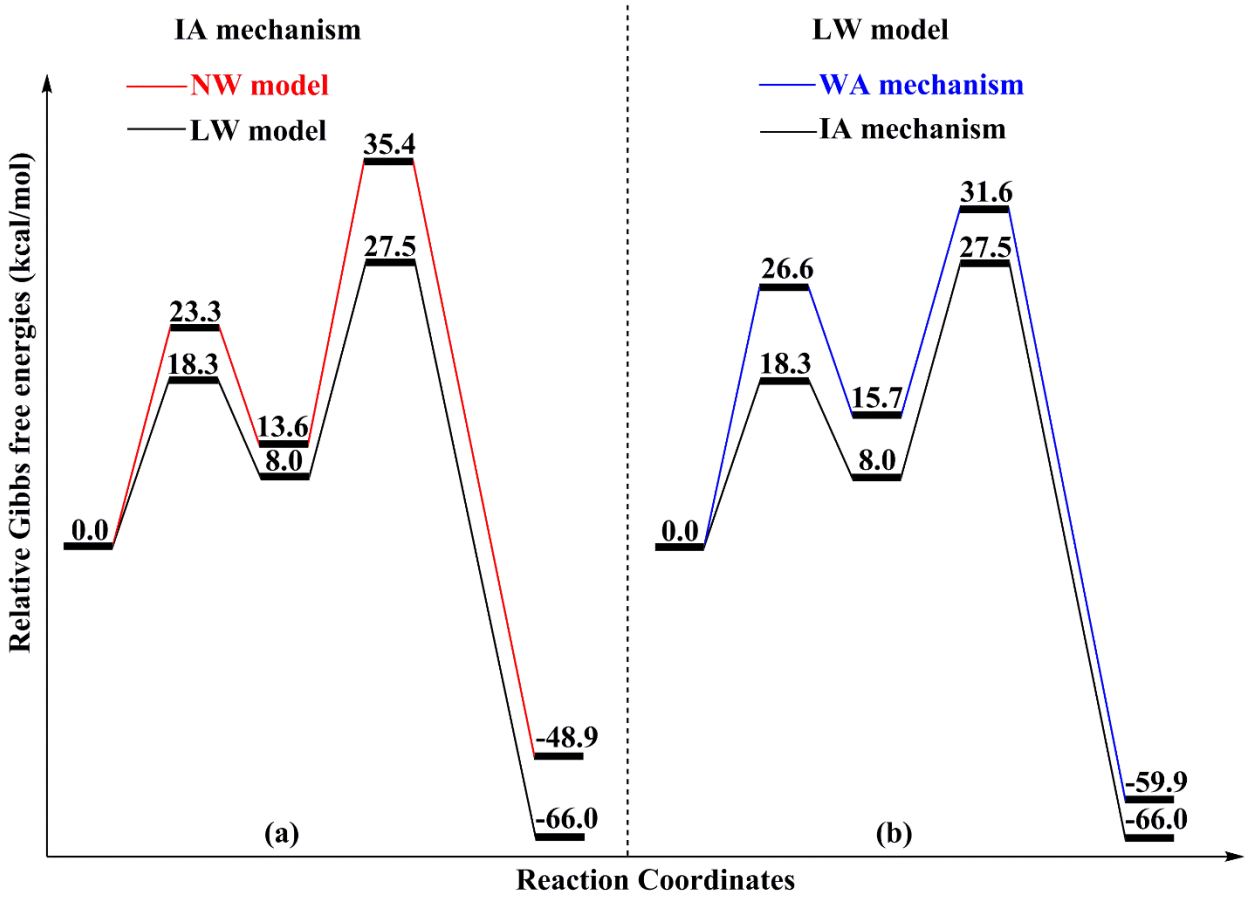

Figure 7: Potential energy diagrams (a) for the IA mechanism (NW and LW models) and (b) IA and WA mechanisms (LW model).

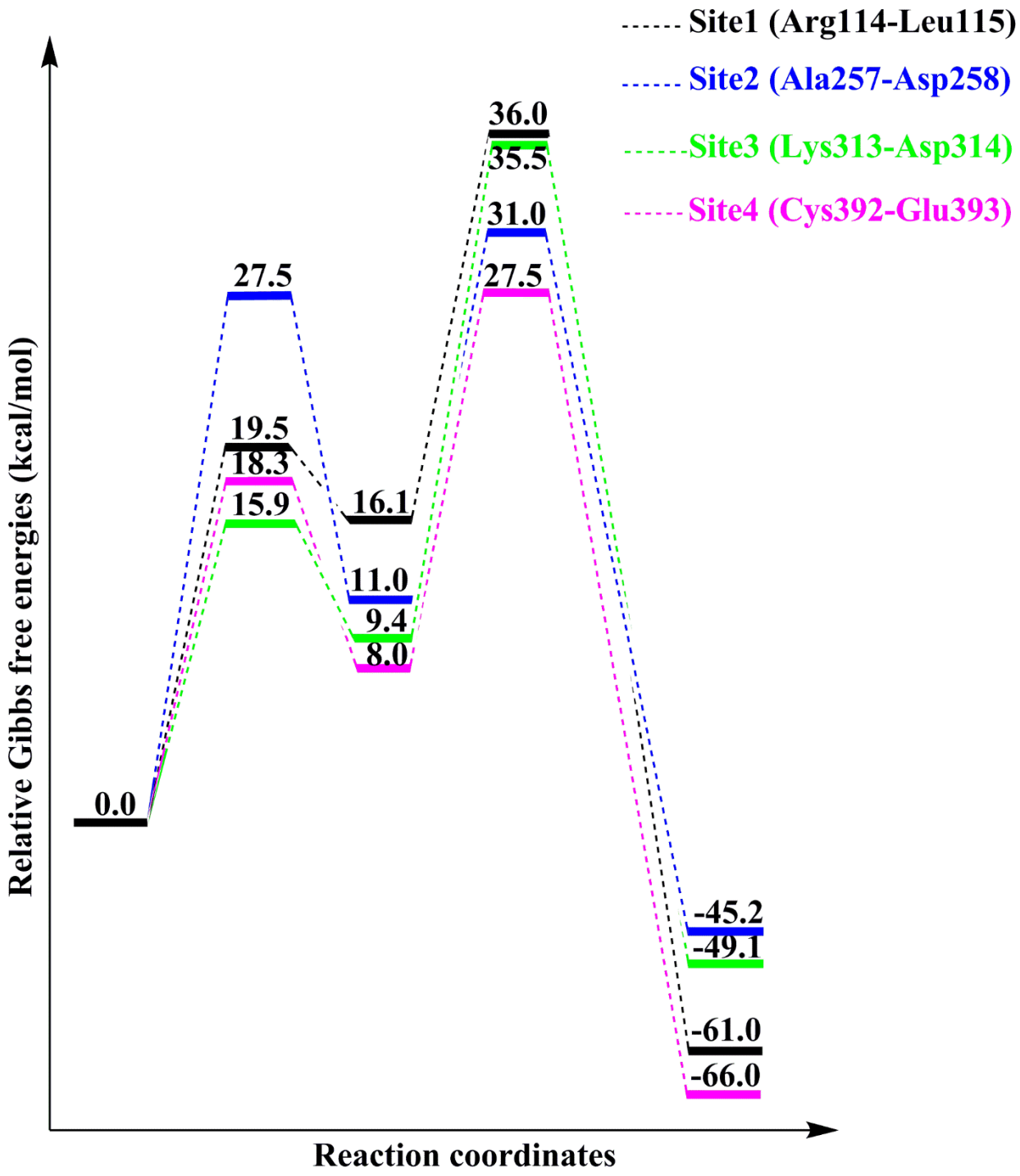

Figure 8: Potential energy surface diagrams for the hydrolysis of all four sites of HSA through IA mechanism (LW model).

References

1. Thomas, J. J., Bakhtiar, R. and Siuzdak, G. *Acc. Chem. Res.* **2000**, *33*, 179-187.
2. Thorner, J., Emr, S. D. and Abelson, J. N. *Meth. Enzymol.* **2000**, *2000*, 326.
3. Wallace, C. J. A. Protein Engineering by Semisynthesis; CRC Press: Boca Raton, Fl., **2000**.
4. Greiner, D. P., Hughes, K. A., Gunasekera, A. H. and Meares, C. F. *Proc. Natl. Acad. Sci. U.S.A.* **1996**, *93*, 71-75.
5. Heyduk, T., Heyduk, E., Severinov, K., Tang, H. and Ebright, R. H. *Proc. Natl. Acad. Sci. U.S.A.* **1996**, *93*, 10162-10166.
6. Colland, F., Fujita, N., Ishihama, A. and Kolb, A. *Genes Cells* **2002**, *7*, 233-247.
7. Cheng, X., Shaltiel, S. and Taylor, S. S. *Biochemistry* **1998**, *37*, 14005-14013.
8. Baichoo, N. and Heyduk, T. *Protein Sci.* **1999**, *8*, 518-528.
9. Loizos, N. *Meth. Enzymol.* **2004**, *261*, 199-210.
10. Mocz, G. *Eur. J. Biochem.* **1989**, *179*, 373-378.
11. Lewis, J. K., Bendahmane, M., Smith, T. J., Beachy, R. N. and Siuzdak, G. *Proc. Natl. Acad. Sci. U.S.A.* **1998**, *95*, 8596-8601.
12. Galante, Y. M. and Formantici, C. *Curr. Org. Chem.* **2003**, *7*, 1399-1422.
13. Suh, J. *Acc. Chem. Res.* **1992**, *25*, 273-278.
14. Lee, T. Y. and Suh, J. *Chem. Soc. Rev.* **2009**, *38*, 1949-1957.
15. Rao, M. B., Tanksale, A. M., Ghatge, M. S. and Deshpande, V. V. *Microbiol. Mol. Biol. Rev.* **1998**, *62*, 597-635.
16. Radzicka, A. and Wolfenden, R. *J. Am. Chem. Soc.* **1996**, *118*, 6105-6109.
17. Bryant, R. A. R. and Hansen, D. E. *J. Am. Chem. Soc.* **1996**, *118*, 5498-5499.
18. Smith, R. M. and Hansen, D. E. *J. Am. Chem. Soc.* **1998**, *120*, 8910-8913.

19. Suh, J., Park, T. H. and Hwang, B. K. *J. Am. Chem. Soc.* **1992**, *114*, 5141-5146.

20. Rana, T. M. and Meares, C. F. *J. Am. Chem. Soc.* **1990**, *112*, 2457-2458.

21. Rana, T. M. and Meares, C. F. *Proc. Natl. Acad. Sci. U.S.A.* **1991**, *88*, 10578-10582.

22. Wu, J., Perrin, D. M., Sigman, D. S. and Kaback, H. R. *Proc. Natl. Acad. Sci. U.S.A.* **1995**, *92*, 9186-9190.

23. Goldshleger, R. and Karlish, S. J. *Proc. Natl. Acad. Sci. U.S.A.* **1997**, *94*, 9596-9601.

24. Ermacora, M. R., Delfino, J. M., Cuenoud, B., Schepartz, A. and Fox, R. O. *Proc. Natl. Acad. Sci. U.S.A.* **1992**, *89*, 6383-6387.

25. Mocz, G. and Gibbons, I. R. *J. Biol. Chem.* **1990**, *265*, 2917-2922.

26. Cremo, C. R., Loo, J. A., Edmonds, C. G. and Hatlelid, K. M. *Biochemistry* **1992**, *31*, 491-497.

27. Grammer, J. C., Loo, J. A., Edmonds, C. G., Cremo, C. R. and Yount, R. G. *Biochemistry* **1996**, *35*, 15582-15592.

28. Zaychikov, E., Martin, E., Denissova, L., Kozlov, M., Markovtsov, V., Kashlev, M., Heumann, H., Nikiforov, V., Goldfarb, A. and Mustaev, A. *Science* **1996**, *273*, 107-109.

29. Gallagher, J., Zelenko, O., Walts, A. D. and Sigman, D. S. *Biochemistry* **1998**, *37*, 2096-2104.

30. Hlavaty, J. J., Benner, J. S., Hornstra, L. J. and Schildkraut, I. *Biochemistry* **2000**, *39*, 3097-3105.

31. Hoyer, D., Cho, H. and Schultz, P. G. *J. Am. Chem. Soc.* **1990**, *112*, 3249-3250.

32. Schepartz, A. and Cuenoud, B. *J. Am. Chem. Soc.* **1990**, *112*, 3247-3249.

33. Cuenoud, B., Tarasow, T. M. and Schepartz, A. *Tetrahedron Lett.* **1992**, *33*, 895-898.

34. Jeon, J. W., Son, S. J., Yoo, C. E., Hong, I. S. and Suh, J. *Bioorg. Med. Chem.* **2003**, *11*, 2901-2910.

35. Kassai, M., Ravi, R. G., Shealy, S. J. and Grant, K. B. *Inorg. Chem.* **2004**, *43*, 6130-6132.

36. Chae, P. S., Kim, M., Jeung, C., Lee, S. D., Park, H., Lee, S. and Suh, J. *J. Am. Chem. Soc.* **2005**, *127*, 2396-2397.

37. Milović, N. M. and Kostić, N. M. *J. Am. Chem. Soc.* **2003**, *125*, 781-788.

38. Buranaprapuk, A., Leach, S. P., Kumar, C. V. and Bocarsly, J. R. *Biochim. Biophys. Acta* **1998**, *1387*, 309-316.

39. Shrivastava, H. Y. and Nair, B. U. *Biochem. Biophys. Res. Commun.* **2001**, *285*, 915-920.

40. Shrivastava, H. Y. and Nair, B. U. *Biochem. Biophys. Res. Commun.* **2000**, *279*, 980-983.

41. Bentley, K. W. and Creaser, E. H. *Biochem. J* **1973**, *135*, 507-511.

42. Bal, W., Lukszo, J., Bialkowski, K. and Kasprzak, K. S. *Chem. Res. Toxicol.* **1998**, *11*, 1014-1023.

43. Bal, W., Liang, R., Lukszo, J., Lee, S. H., Dizdaroglu, M. and Kasprzak, K. S. *Chem. Res. Toxicol.* **2000**, *13*, 616-624.

44. Manka, S., Becker, F., Hohage, O. and Sheldrick, W. S. *J. Inorg. Biochem.* **2004**, *98*, 1947-1956.

45. Erxleben, A. *Inorg. Chem.* **2005**, *44*, 1082-1094.

46. Kumar, C. V. and Thota, J. *Inorg. Chem.* **2005**, *44*, 825-827.

47. Rivas, J. C. M., Salvagni, E., Prabaharan, R., Rosales, R. T. M. and Parsons, S. *Dalton Trans.* **2004**, 172-177.

48. Murthy, N. N., Mahroof-Tahir, M. and Karlin, K. D. *J. Am. Chem. Soc.* **1993**, *115*, 10404-10405.

49. Milovic, N. M., Dutca, L.-M. and Kostic, N. M. *Chem. Eur. J.* **2003**, *9*, 5097-5106.

50. Sutton, P. A. and Buckingham, D. A. *Acc. Chem. Res.* **1987**, *20*, 357-364.

51. Protas, A. M., Bonna, A., Kopera, E. and Bal, W. *J. Inorg. Biochem.* **2011**, *105*, 10-16.

52. Krężel, A., Kopera, E., Protas, A. M., Poznański, J., Wysłouch-Cieszyńska, A. and Bal, W. *J. Am. Chem. Soc.* **2010**, *132*, 3355-3366.

53. Rajkovic, S., Zivkovic, M. D., Kallay, C., Sovago, I. and Djuran, M. I. *Dalton Trans.* **2009**, *39*, 8370-8377.

54. Hong, J., Jiao, Y., He, W., Guo, Z., Yu, Z., Zhang, J. and Zhu, L. *Inorg. Chem.* **2010**, *49*, 8148-8154.

55. Grant, K. and Kassai, M. *Curr. Org. Chem.* **2006**, *10*, 1035-1049.

56. Szajna-Fuller, E., Ingle, G. K., Watkins, R. W., Arif, A. M. and Berreau, L. M. *Inorg. Chem.* **2007**, *46*, 2353-2355.

57. Menger, F. M. and Ladika, M. *J. Am. Chem. Soc.* **1988**, *110*, 6794-6796.

58. Stroobants, K., Absillis, G., Moelants, E., Proost, P. and Parac-Vogt, T. N. *Chem. Eur. J.* **2014**, *20*, 3894-3897.

59. Stroobants, K., Goovaerts, V., Absillis, G., Bruylants, G., Moelants, E., Proost, P. and Parac-Vogt, T. N. *Chem. Eur. J.* **2014**, *20*, 9567-9577.

60. Judd, D. A., Nettles, J. H., Nevins, N., Snyder, J. P., Liotta, D. C., Tang, J., Ermolieff, J., Schinazi, R. F. and Hill, C. L. *J. Am. Chem. Soc.* **2001**, *123*, 886-897.

61. Sap, A., Absillis, G. and Parac-Vogt, T. N. *Dalton Trans.* **2015**, *44*, 1539-1548.

62. Vanhaecht, S., Absillis, G. and Parac-Vogt, T. N. *Dalton Trans.* **2012**, *41*, 10028-10034.

63. Ly Hong Giang, T., Absillis, G., Bajpe Sneha, R., Martens Johan, A. and Parac-Vogt Tatjana, N. *Eur. J. Inorg. Chem.* **2013**, *2013*, 4601-4611.

64. Ly, H. G. T., Absillis, G. and Parac-Vogt, T. N. *Dalton Trans.* **2013**, *42*, 10929-10938.

65. Stroobants, K., Moelants, E., Ly, H. G. T., Proost, P., Bartik, K. and Parac-Vogt, T. N. *Chem. Eur. J.* **2013**, *19*, 2848-2858.

66. Ly, H. G. T. and Parac-Vogt, T. N. *ChemPhysChem* **2017**, *18*, 2451-2458.

67. Sap, A., Van Tichelen, L., Mortier, A., Proost, P. and Parac-Vogt, T. N. *Eur. J. Inorg. Chem.* **2016**, *2016*, 5098-5105.

68. Proust, A., Thouvenot, R. and Gouzerh, P. *Chem. Commun.* **2008**, 1837-1852.

69. Long, D.-L., Tsunashima, R. and Cronin, L. *Angew. Chem. Int. Ed.* **2010**, *49*, 1736-1758.

70. Pope, M. Heteropoly and Isopoly Oxometalates; Springer: Verlag Berlin Heidelberg, **1983**.

71. Pope, M. T. and Müller, A. *Angew. Chem., Int. Ed. Engl.* **1991**, *30*, 34-48.

72. Bard, A., Stratmann, M., Scholz, F. and Pickett, C. Electrochemistry of Isopoly and Heteropoly Oxometalates; Wiley: In Encyclopedia of Electrochemistry, **2006**, pp 607-700.

73. Baker, L. C. W. and Glick, D. C. *Chem. Rev.* **1998**, *98*, 3-50.

74. Kozhevnikov, I. V. *Chem. Rev.* **1998**, *98*, 171-198.

75. Zhang, G., Yang, W. and Yao, J. *Adv. Funct. Mater.* **2005**, *15*, 1255-1259.

76. Zhang, G., Chen, Z., He, T., Ke, H., Ma, Y., Shao, K., Yang, W. and Yao, J. *J. Phys. Chem. B* **2004**, *108*, 6944-6948.

77. Yamase, T. *Chem. Rev.* **1998**, *98*, 307-326.

78. Olson, R. E. and Christ, D. D. *Annu. Rep. Med. Chem.* **1996**, *31*, 327-336.

79. He, X. M. and Carter, D. C. *Nature* **1992**, *358*, 209-215.

80. Carter, D. C. and Ho, J. X. *Adv. Protein Chem.* **1994**, *45*, 153-203.

81. Peters, T. All About Albumin; Academic Press: New York, **1996**.

82. Boglio, C., Hasenknopf, B., Lenoble, G., Rémy, P., Gouzerh, P., Thorimbert, S., Lacôte, E., Malacria, M. and Thouvenot, R. *Chem. Eur. J.* **2008**, *14*, 1532-1540.

83. Dupré, N., Rémy, P., Micoine, K., Boglio, C., Thorimbert, S., Lacôte, E., Hasenknopf, B. and Malacria, M. *Chem. Eur. J.* **2010**, *16*, 7256-7264.

84. Parac-Vogt, T. N., Vandebroek, L., De Zitter, E., Ly Thi, H. G., Conić, D., Mihaylov, T., Meervelt, L. V., Pierloot, K., Proost, P. and Sap, A. *Chem. Eur. J.* **2018**, *published online*.

85. Goovaerts, V., Stroobants, K., Absillis, G. and Parac-Vogt, T. N. *Phys. Chem. Chem. Phys.* **2013**, *15*, 18378-18387.

86. Sap, A., De Zitter, E., Van Meervelt, L. and Parac-Vogt, T. N. *Chem. Eur. J.* **2015**, *21*, 11692-11695.

87. Baroni, S., Mattu, M., Vannini, A., Cipollone, R., Aime, S., Ascenzi, P. and Fasano, M. *Eur. J. Biochem.* **2001**, *268*, 6214-6220.

88. di Masi, A., Gullotta, F., Bolli, A., Fanali, G., Fasano, M. and Ascenzi, P. *FEBS J.* **2011**, *278*, 654-662.

89. Fanali, G., Cao, Y., Ascenzi, P., Trezza, V., Rubino, T., Parolaro, D. and Fasano, M. *IUBMB Life* **2011**, *63*, 446-451.

90. Fasano, M., Curry, S., Terreno, E., Galliano, M., Fanali, G., Narciso, P., Notari, S. and Ascenzi, P. *IUBMB Life* **2005**, *57*, 787-796.

91. SUDLOW, G., BIRKETT, D. J. and WADE, D. N. *Mol. Pharmacol.* **1975**, *11*, 824-832.

92. SUDLOW, G., BIRKETT, D. J. and WADE, D. N. *Mol. Pharmacol.* **1976**, *12*, 1052-1061.

93. Zheng, L., Ma, Y., Zhang, G., Yao, J., Keita, B. and Nadjo, L. *Phys. Chem. Chem. Phys.* **2010**, *12*, 1299-1304.

94. Zhang, G., Keita, B., Craescu, C. T., Miron, S., de Oliveira, P. and Nadjo, L. *J. Phys. Chem. B* **2007**, *111*, 11253-11259.

95. Zhang, G., Keita, B., Craescu, C. T., Miron, S., de Oliveira, P. and Nadjo, L. *Biomacromolecules* **2008**, *9*, 812-817.

96. Lopez, X., Carbo, J. J., Bo, C. and Poblet, J. M. *Chem. Soc. Rev.* **2012**, *41*, 7537-7571.

97. López, X., Miró, P., Carbó, J. J., Rodríguez-Fortea, A., Bo, C. and Poblet, J. M. *Theor. Chem. Acc.* **2011**, *128*, 393-404.

98. Solé-Daura, A., Goovaerts, V., Stroobants, K., Absillis, G., Jiménez-Lozano, P., Poblet, J. M., Hirst, J. D., Parac-Vogt, T. N. and Carbó, J. J. *Chem. Eur. J.* **2016**, *22*, 15280-15289.

99. Wilcox, D. E. *Chem. Rev.* **1996**, *96*, 2435-2458.

100. Hegg, E. L. and Burstyn, J. N. *Coord. Chem. Rev.* **1998**, *173*, 133-165.

101. Parkin, G. *Chem. Rev.* **2004**, *104*, 699-768.

102. Weston, J. *Chem. Rev.* **2005**, *105*, 2151-2174.

103. Vicente, J. and Arcas, A. *Coord. Chem. Rev.* **2005**, *249*, 1135-1154.

104. Breslow, R. and Dong, S. D. *Chem. Rev.* **1998**, *98*, 1997-2012.

105. Chin, J. *Acc. Chem. Res.* **1991**, *24*, 145-152.

106. Chin, J. and Kim, H. In Artificial Enzymes; Wiley-VCH Verlag GmbH and Co. KGaA, **2006**, p 133-157.

107. Suh, J. *Acc. Chem. Res.* **2003**, *36*, 562-570.

108. Elton, E. S., Zhang, T., Prabhakar, R., Arif, A. M. and Berreau, L. M. *Inorg. Chem.* **2013**, *52*, 11480-11492.

109. Zhang, T., Ozbil, M., Barman, A., Paul, T. J., Bora, R. P. and Prabhakar, R. *Acc. Chem. Res.* **2015**, *48*, 192-200.

110. Kumar, A., Zhu, X., Walsh, K. and Prabhakar, R. *Inorg. Chem.* **2010**, *49*, 38-46.

111. Zhang, T., Zhu, X. and Prabhakar, R. *J. Phys. Chem. B* **2014**, *118*, 4106-4114.

112. Wezynfeld, N. E., Frączyk, T. and Bal, W. *Coord. Chem. Rev.* **2016**, *327–328*, 166-187.

113. Krämer, R. *Coord. Chem. Rev.* **1999**, *182*, 243-261.

114. Chin, J. and Kim, H.-J. Artificial Enzymes; Wiley-Vch: Weinheim, **2005**.

115. Breslow, R. and Zhang, B. *J. Am. Chem. Soc.* **1992**, *114*, 5882-5883.

116. Breslow, R. and Zhang, B. *J. Am. Chem. Soc.* **1994**, *116*, 7893-7894.

117. Breslow, R., Zhang, X., Xu, R., Maletic, M. and Merger, R. *J. Am. Chem. Soc.* **1996**, *118*, 11678-11679.

118. Suh, J. *Acc. Chem. Res.* **2003**, *36*, 562-570.

119. Guthrie, J. P. *J. Am. Chem. Soc.* **1977**, *99*, 3991-4001.

120. Johnson, J. S. and Evans, D. A. *Acc. Chem. Res.* **2000**, *33*, 325-335.

121. Pfaltz, A. *Acc. Chem. Res.* **1993**, *26*, 339-345.

122. Daver, H., Das, B., Nordlander, E. and Himo, F. *Inorg. Chem.* **2016**, *55*, 1872-1882.

123. Daumann, L. J., Schenk, G., Ollis, D. L. and Gahan, L. R. *Dalton Trans.* **2014**, *43*, 910-928.

124. Mitić, N., Smith, S. J., Neves, A., Guddat, L. W., Gahan, L. R. and Schenk, G. *Chem. Rev.* **2006**, *106*, 3338-3363.

125. Neves, A., Lanznaster, M., Bortoluzzi, A. J., Peralta, R. A., Casellato, A., Castellano, E. E., Herrald, P., Riley, M. J. and Schenk, G. *J. Am. Chem. Soc.* **2007**, *129*, 7486-7487.

126. Jarenmark, M., Csapo, E., Singh, J., Wockel, S., Farkas, E., Meyer, F., Haukka, M. and Nordlander, E. *Dalton Trans.* **2010**, *39*, 8183-8194.

127. Jarenmark, M., Kappen, S., Haukka, M. and Nordlander, E. *Dalton Trans.* **2008**, 993-996.

128. Lee, L., Berg, D. J. and Bushnell, G. W. *Organometallics* **1997**, *16*, 2556-2561.

129. Luong, T. K. N., Absillis, G., Shestakova, P. and Parac-Vogt, T. N. *Eur. J. Inorg. Chem.* **2014**, *2014*, 5276-5284.

130. Ly, H. G. T., Absillis, G. and Parac-Vogt, T. N. *New J. Chem.* **2016**.

131. Sap, A., De Zitter, E., Van Meervelt, L. and Parac-Vogt, T. N. *Chem. Eur. J.* **2015**, *21*, 11692-11695.

132. Stroobants, K., Goovaerts, V., Absillis, G., Bruylants, G., Moelants, E., Proost, P. and Parac-Vogt, T. N. *Chem. Eur. J.* **2014**, *20*, 9567-9577.

133. Kassai, M., Ravi, G. and Grant, K. 55th Southeast Regional Meeting of the American Chemical Society, Atlanta, GA, United States, November 16-19 2003, pp 449.

134. Wilkinson, G., Gillard, R. D. and McCleverty, J. A. Comprehensive coordination chemistry : the synthesis, reactions, properties and applications of coordination compounds; Pergamon Press: Oxford, England ; New York, **1987**.

135. Ghosh, S., Sharma, A. and Talukder, G. *Biol. Trace Elem. Res.* **1992**, *35*, 247-271.

136. Singhal, A., Toth, L. M., Lin, J. S. and Affholter, K. *J. Am. Chem. Soc.* **1996**, *118*, 11529-11534.

137. Ly, H. G. T., Absillis, G. and Parac-Vogt, T. N. *New J. Chem.* **2016**, *40*, 976-984.

138. Kim, J. H., Britten, J. and Chin, J. *J. Am. Chem. Soc.* **1993**, *115*, 3618-3622.

139. Chin, J. and Zou, X. *J. Am. Chem. Soc.* **1984**, *106*, 3687-3688.

140. Chei, W., Ju, H. and Suh, J. *J. Biol. Inorg. Chem.* **2011**, *16*, 511-519.

141. Lipscomb, W. N. and Sträter, N. *Chem. Rev.* **1996**, *96*, 2375-2434.

142. Christianson, D. W. and Lipscomb, W. N. *Acc. Chem. Res.* **1989**, *22*, 62-69.

143. Coleman, F., Hynes, M. J. and Erxleben, A. *Inorg. Chem.* **2010**, *49*, 6725-6733.

144. Pearson, R. G. **1968**, *45*, 581-587.

145. Pearson, R. G. Chemical Hardness; Wiley-VCH, **1997**.

146. Breslow, R., Ed. Artifical Enzymes; Wiley-VCH: New York, **2005**.

147. Burgess, J. Metal ions in solution; Halsted Press (Wiley): New York, **1978**, pp 259.

148. Bertini, I., Luchinat, C., Rosi, M., Sgamellotti, A., and Tarantelli, F. *Inorg. Chem.* **1990**, *29*, 1460-1463.

149. Toyofumi, I., Yuki, F., Toshiji, T., Yuzo, Y. and Hiroyuki, H. *Bull. Chem. Soc. Jpn.* **1996**, *69*, 1265-1274.

150. Itoh, T., Hisada, H., Usui, Y. and Fujii, Y. *Inorg. Chim. Acta* **1998**, *283*, 51-60.

151. Koike, T. and Kimura, E. *J. Am. Chem. Soc.* **1991**, *113*, 8935-8941.

152. Bonfá, L., Gatos, M., Mancin, F., Tecilla, P. and Tonellato, U. *Inorg. Chem.* **2003**, *42*, 3943-3949.

153. Frisch, M. J., Trucks, G. W., Schlegel, H. B., Scuseria, G. E., Robb, M. A., Cheeseman, J. R., Scalmani, G., Barone, V., Mennucci, B., Petersson, G. A., Nakatsuji, H., Caricato, M., Li, X., Hratchian, H. P., Izmaylov, A. F., Bloino, J., Zheng, G., Sonnenberg, J. L., Hada, M., Ehara, M., Toyota, K., Fukuda, R., Hasegawa, J., Ishida, M., Nakajima, T., Honda, Y., Kitao, O., Nakai, H., Vreven, T., Montgomery, J., J. A.; , Peralta, J. E., Ogliaro, F., Bearpark, M., Heyd, J. J., Brothers, E., Kudin, K. N., Staroverov, V. N., Kobayashi, R., Normand, J., Raghavachari, K., Rendell, A., Burant, J. C., Iyengar, S. S., Tomasi, J., Cossi, M., Rega, N., Millam, N. J., Klene, M., Knox, J. E., Cross, J. B., Bakken, V., Adamo, C., Jaramillo, J., Gomperts, R., Stratmann, R. E., Yazyev, O., Austin, A. J., Cammi, R., Pomelli, C., Ochterski, J. W., Martin, R. L., Morokuma, K., Zakrzewski, V. G., Voth, G. A., Salvador, P., Dannenberg, J. J., Dapprich, S., Daniels, A. D., Farkas, Ö., Foresman, J. B., Ortiz, J. V., Cioslowski, J. and Fox, D. J.; Gaussian, Inc.: Wallingford CT, 2009.

154. Senn Hans, M. and Thiel, W. *Angew. Chem. Int. Ed.* **2009**, *48*, 1198-1229.

155. Chung, L. W., Sameera, W. M. C., Ramozzi, R., Page, A. J., Hatanaka, M., Petrova, G. P., Harris, T. V., Li, X., Ke, Z., Liu, F., Li, H.-B., Ding, L. and Morokuma, K. *Chem. Rev.* **2015**, *115*, 5678-5796.

156. Vreven, T., Morokuma, K., Farkas, Ö., Schlegel, H. B. and Frisch, M. J. *J. Comp. Chem.* **2003**, *24*, 760-769.

157. Becke, A. D. *Phys. Rev. A* **1988**, *38*, 3098-3100.

158. Becke, A. D. *J. Chem. Phys.* **1993**, *98*, 5648-5652.

159. Hay, P. J. and Wadt, W. R. *J. Chem. Phys.* **1985**, *82*, 270-283.

160. Ponder, J. W. and Case, D. A. *Adv. Protein Chem.* **2003**, *66*, 27-85.

161. Yong, D., Chun, W., Shibasish, C., C., L. M., Guoming, X., Wei, Z., Rong, Y., Piotr, C., Ray, L., Taisung, L., James, C., Junmei, W. and Peter, K. *J. Comput. Chem.* **2003**, *24*, 1999-2012.

162. Sap, A., De Zitter, E., Van Meervelt, L. and Parac-Vogt, T. N. *Chem. Eur. J.* **2015**, *21*, 11692-11695.

163. Wang, Y., Yu, H., Shi, X., Luo, Z., Lin, D. and Huang, M. *J. Biol. Chem.* **2013**, *288*, 15980-15987.

164. Zhang, T., Sharma, G., Paul, T. J., Hoffmann, Z. and Prabhakar, R. *J. Chem. Inf. Model.* **2017**, *57*, 1079-1088.

165. Zhang, T., Zhu, X. and Prabhakar, R. *Organometallics* **2014**, *33*, 1925-1935.

166. Bora, R., Ozbil, M. and Prabhakar, R. *J. Biol. Inorg. Chem.* **2010**, *15*, 485-495.